Organic & Biomolecular Chemistry

Accepted Manuscript

ROYAL SOCIETY OF CHEMISTRY

www.rsc.org/obc

Journal Name

RSCPublishing

ARTICLE

A highly selective ratiometric bifunctional fluorescence probe for Hg^{2+} and F^- ions

Cite this: DOI: 10.1039/xoxxoooooox

Qing-Wen Xu, Chen Wang, Zuo-Bang Sun and Cui-Hua Zhao*

Received ooth January 2012,
Accepted ooth January 2012

DOI: 10.1039/xoxxoooooox

www.rsc.org/

A triarylborane derivative **BN-S**, which contains both a Hg^{2+}-responsive dithioacetal group and a F^--responsive boryl group, has been designed and synthesized via the functionalization of 2-dimesitylboryl-2′-(N,N-dimethylamino)biphenyl core skeleton with dithioacetal substituent. This compound displays intense intramolecular charge transfer fluorescence, even for its nano-aggregates in water. The Hg^{2+}-promoted deprotection of dithioacetal group and complexation of F^- with tri-coordinate boron center cause hypochromism of fluorescence in different extents. And thus **BN-S** can behave as a promising ratiometric bifunctional fluorescence probe to detect Hg^{2+} and F^- simultaneously. In addition, the detection of Hg^{2+} is performable in an aqueous medium using its nano-aggregates.

Introduction

The sensitive and selective detection of various ionic analytes has been the subject of strong interest because of their widespread uses and the subsequent pollution triggering severe health and environmental problems.[1] For instance, mercury is one of the most toxic heavy elements and is easily bioaccumulated in the body due to its durability.[2] The accumulation of mercury in the human body can lead to various cognitive and motor disorders and Minamata disease.[3] On the other hand, fluoride anions play important roles in dental care, treatment of osteoporosis, fluorination of water supplies.[4] High doses of this anion are, however, dangerous and can result in various ailments, such as fluorosis, nephrotoxic changes and urolithiais.[5] To detect anionic fluoride and cationic mercury ions, fluorescence sensing is one of the most powerful methods owing to its high sensitivity and the simplicity of the equipment requirement.[6] It is well known that the traditional fluorescence intensity-based methodology is easily interfered by sensor concentration, photo bleaching, and illumination intensity. To eliminate these unfavorable effects, it is highly desirable to develop ratiometric fluorescence probes,[7,8] which use the ratios of the fluorescence intensities at two different wavelengths, allowing precise and quantitative analysis and imaging even in complicated systems. In addition, most of the attention has been focused on the monofunctional fluorescence anion or cation sensors. The chemosensors that are suitable for simultaneous detection of multiple analytes have only very recently attracted great notice.[9] To the best of our knowledge, the examples for individual detection of both Hg^{2+} and F^- ions are still quite limited.[10] In this context, it is still a challenging and meaningful issue to design ratiometric bifunctional fluorescence probe for Hg^{2+} and F^- ions.

To realize fluoride sensing, the specific Lewis acid/base interactions between the tri-coordinate boron center of triarylboranes and fluoride ions have been proved to be an efficient strategy.[11] One of the most intriguing features of triarylboranes is the p_π-π^* conjugation between the vacant p orbital on boron center and the π^* orbital of the attached π-conjugated framework.[12] The complexation of tri-coordinate boron center with fluoride anions would disrupt the p_π-π^* conjugation and lead to remarkable changes in UV/Vis absorption, fluorescence, two-photon absorption and excited fluorescence.[13–20] Interestingly, the triarylboranes generally possess high selectivity for fluoride over other anions such as chloride, bromide and iodide, as the result of the steric hindrance of bulky substituents on boron center, which not only ensures stability to water including moisture but also prevents complexation with other larger Lewis bases. Despite the large number of triarylboranes capable of fluoride sensing, those that can behave as bifunctional probes are very rare,[21] which might be ascribed to the difficulty in the introduction of other ion-responsive functional groups in triarylboranes. In continuation of our research on triarylboranes-based functional materials, we have recently disclosed a new class of intramolecular charge-transfer (ICT) emitting triarylborane, in which the electron-donating dimethylamino group and the electron-accepting boryl group were introduced at the *o*,*o*′-positions of flexible biphenyl framework.[22] The coordination with fluoride can lead to 165 nm blue shift in the fluorescence, enabling ratiometric fluorescence sensing of fluoride. It is notable that the *para*-position of amino group is very reactive towards electrophilic substitution and thus it is possible to introduce various substituents and finely tune the photophysical properties.[22c] Encouraged by these facts, we have now designed and synthesized a simple but novel triarylborane **BN-S**, in which

thioacetal group was introduced at *para*-position of amino in the 2-dimesitylboryl-2'-(N,N-dimethylamino)biphenyl core unit. In this molecular design, the dithioacetal group was introduced because the specific Hg^{2+}-promoted thioacetal deprotection reaction to generate formyl group has been well utilized for the design of Hg^{2+} probes.[23] We envisioned that the formylated compound **BN-CHO** (Scheme 1), produced by the Hg^{2+}-promoted thioacetal deprotection of **BN-S**, might display photophysical properties different from those of **BN-S** due to stronger electron-accepting ability of formyl than dithioacetal group. As a result, **BN-S** would be able to detect Hg^{2+} in addition to F^- ions. We indeed found that **BN-S** exhibits blue shift in fluorescence in different extents upon reaction with F^- and Hg^{2+}, demonstrating its great utility for the simultaneous and ratiometric fluorescence sensing of both Hg^{2+} and F^- ions. Moreover, **BN-S** is still intensely emissive in aggregate state and thus the detection of Hg^{2+} can be performed using its nano-aggregates formed in aqueous medium.

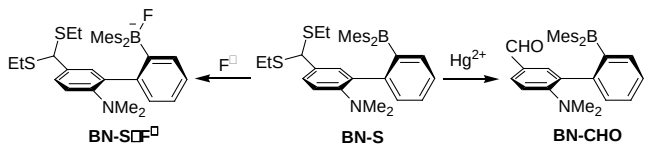

Scheme 1. The design concept of **BN-S**.

Results and discussion

Synthesis and photophysical properties

As illustrated in Scheme 2, the target compound **BN-S** was easily synthesized via a one-step reaction from **BN-CHO**, which was previously prepared through electrophilic formylation of 2-dimesitylboryl-2'-(N,N-dimethylamino)biphenyl core unit.[22c] In the presence of P_2O_5/SiO_2, the straightforward protection of the formyl group with ethanethiol proceeded smoothly at 40 °C to provide **BN-S** in 87% yield. **BN-S** is very stable in air and can be purified by silica gel column chromatography. And its structure was fully characterized by ^1H and ^{13}C NMR spectroscopy and high-resolution mass spectrometry.

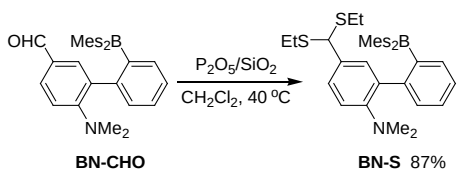

Scheme 2 Synthesis of **BN-S**.

The UV/vis absorption and fluorescence spectra of **BN-S** are shown in Fig. 1 and the related data are summarized in Table 1. The photophysical properties of **BN-S** are very similar to the core skeleton, 2-dimesitylboryl-2'-(N,N-dimethylamino)biphenyl,[22a] which might be ascribed to the weak electronic effect of dithioacetal group. And thus in cyclohexane, **BN-S** displays an intense absorption at 312 nm (log ε = 4.09) and yellowish green fluorescence at 523 nm (Φ_F = 0.17). In addition, the fluorescence spectra exhibit large solvatochromism from 523 nm in cyclohexane to 585 nm in acetonitrile while no obvious solvent dependence was observed in absorption. The large solvatochromism on fluorescence clearly suggests the intramolecular charge-transfer (ICT) character of **BN-S**. Another noteworthy characteristic feature of **BN-S** is that it still shows bright greenish yellow emission in the powder form, indicating its great fluorescence property in the condensed state. This phenomenon encouraged us to investigate its photophysical properties of **BN-S** in aggregates in aqueous medium, the intense fluorescence of which would enable the fluorescence sensing of ions in aqueous medium. The nano-aggregates of **BN-S** were prepared via the rapid injection of its solution in THF (1 mL, 5.26 mM) into 100 mL water. In view of the spectra, the absorption retains almost unchanged compared with those in solutions and the fluorescence is only slightly red shifted compared with that in cyclohexane, suggesting the weak intermolecular interactions in the aggregate state. Although the fluorescence efficiency of nano-aggregates in aqueous medium (Φ_F = 0.05) decreases to some extent compared with those of solution in organic solvents, the fluorescence is still high enough for the fluorescence sensing. The time-resolved fluorescence study

Table 1. UV/vis absorption and fluorescence data of **BN-S**.

	solvent	λ_{abs}[a]/nm (log ε)	λ_{em}/nm (Φ_F)[b]	τ /ns	k_r /s^{-1}	k_{nr} /s^{-1}
BN-S	cyclohexane	312 (4.09)	523 (0.17)	–	–	–
	benzene	310 (4.08)	546 (0.16)	–	–	–
	$CHCl_3$	304 (4.08)	550 (0.14)	–	–	–
	THF	308 (4.07)	569 (0.12)	25.7	4.67×10^6	3.42×10^7
	MeCN	306 (4.04)	585 (0.08)	–	–	–
	H_2O[c]	310 (3.93)	534 (0.05)	39.0	1.28×10^6	2.44×10^7
BN-CHO	H_2O[d]	332 (4.03)	503 (0.08)	9.3/19.3 (60/40)[e]	–	–
BN-S•F⁻	THF	–	395 (0.11)	0.94	1.17×10^8	9.46×10^8

[a] Only the longest maxima are shown. [b] Calculated using fluorescein as standard. [c] The nano-aggregates were prepared via the rapid injection of a solution of **BN-S** in THF (1 mL, 5.26 mM) into 100 mL H_2O under vigorous stirring for 30 s. [d] The nano-aggregates were prepared via the rapid injection of a solution of **BN-CHO** in THF (100 μL, 5.26 mM) into 10 mL H_2O under vigorous stirring for 30 s. [e] Amplitudes of two lifetimes given in parentheses.

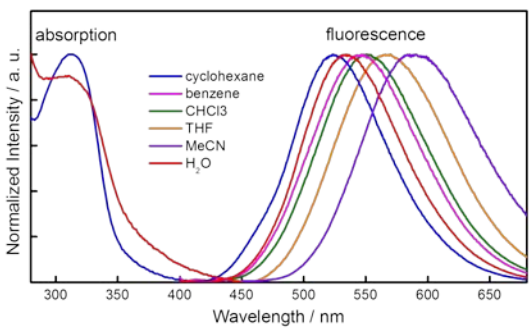

Fig. 1 UV/vis absorption and fluorescence spectra of **BN-S**.

showed that the fluorescence lifetime becomes much longer from THF solution to the nano-aggregates in aqueous medium and the decrease in the fluorescence efficiency is mainly ascribed to the deceleration of the radiative decay process (Table 1).

Optical response of BN-S to Hg^{2+}

Considering the high fluorescence intensity of **BN-S** in water and the fact that Hg^{2+} is widely distributed in aqueous medium, the UV/vis absorption and emission spectra changes of **BN-S** were first examined for its nano-aggregates in water (52.6 μM) to evaluate its recognition ability towards Hg^{2+}. As shown in Fig. 2, the addition of 30 equiv. Hg^{2+} induced 22 nm bathochromism of absorption from 310 nm to 332 nm. In contrast, the emission is blue shifted by 31 nm from 534 nm to 503 nm. It was noted that the absorption and fluorescence spectra of **BN-S** with excess amount of Hg^{2+} are almost identical to those of **BN-CHO**, which implied that the Hg^{2+}-promoted deprotection of **BN-S** proceeded smoothly to generate **BN-CHO**. The transformation of **BN-S** to **BN-CHO** was further confirmed by ^{1}H NMR measurement. As shown in Fig. 3, upon addition of Hg^{2+} cations, the ^{1}H NMR of **BN-S** dramatically changed. The characteristic signal at 4.97 ppm corresponding to thioacetal proton completely disappeared, which was accompanied by the appearance of CHO signal at 9.55 ppm. Notably, the fluorescence quantum yield increased to 0.08 once **BN-S** was converted to **BN-CHO**, which was accompanied by the shortening of fluorescence lifetime (Table 1).

The remarkable blue shift of the fluorescence maximum wavelength of **BN-S** upon reaction with Hg^{2+} suggests its potential utility as the ratiometric fluorescent probe for Hg^{2+}. To further explore this point, the time-dependent fluorescence spectra of **BN-S** were measured. As shown in Fig. 4, the fluorescence ratio between 503 nm and 534 nm (I_{503}/ I_{534}) increased gradually along with the time consuming and reached maximum after about 5 min, denoting the rapid reaction of **BN-S** towards Hg^{2+}. In addition, the pH effect was also examined since thioacetal is a pH sensitive group (Fig. S-1). Although **BN-S** decomposes slightly in acidic conditions over a long period (ca. 10 hours), I_{503}/ I_{534} is almost independent of pH within the measurement time scales. In the presence of excess amount of Hg^{2+}, the fluorescence ratio (I_{503}/ I_{534}) is highest when the pH is around 6.0. And in the unbuffered water, the fluorescence ratio (I_{503}/ I_{534}) is very close to the highest value. The drop of the fluorescence ratio (I_{503}/ I_{534}) in the neutral or basic conditions might be ascribed to the formation of $Hg(OH)_2$.

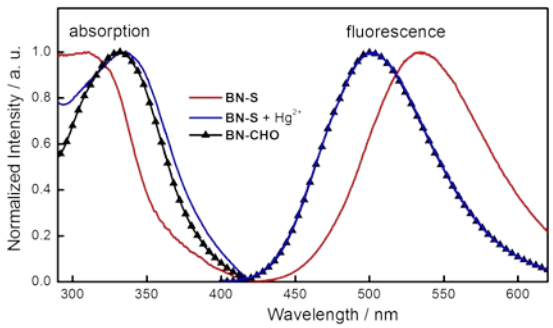

Fig. 2 UV/vis absorption and fluorescence spectra (λ_{ex} = 320 nm) of nano-aggregates of **BN-CHO** (52.6 μM) in water, and **BN-S** (52.6 μM) in water in the absence and presence of 30 equiv. of Hg^{2+} (chloride salt).

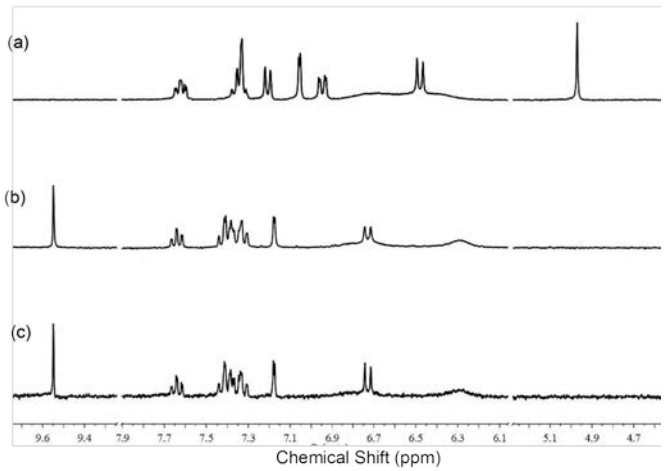

Fig. 3 Partial ^{1}H NMR spectra (300 MHz, d_6-DMSO) of (a) **BN-S**, (b) **BN-S** with $HgCl_2$ and (c) **BN-CHO**.

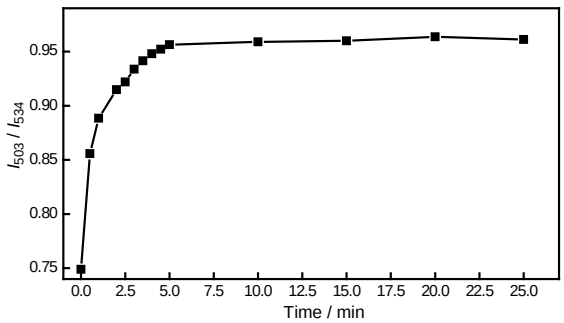

Fig. 4 Time-dependent fluorescence ratio (I_{503} / I_{534}) changes of **BN-S** in water (52.6 μM) in the presence of 1 equiv. of Hg^{2+} (chloride salt).

Considering prompt fluorescence response and remarkable blue shift of the fluorescence maximum wavelength of **BN-S** upon reaction with Hg^{2+}, the detailed sensing performance of **BN-S** for Hg^{2+} has been investigated mainly by fluorescence spectroscopy in unbuffered water. As shown in Fig. 5, **BN-S** displays an intense greenish yellow fluorescence at 534 nm for its nano-aggregates in aqueous media. With the increasing addition of Hg^{2+}, this band was displaced gradually by a hypochromic band at 503 nm, which is characteristic of **BN-CHO**. The fluorescence intensity ratios between 503 and 534 nm (I_{503}/ I_{534}) increased from 0.69–1.12 with the gradual increment of Hg^{2+} concentration. It was interesting to find that excellent linear relationship was obtained between I_{503}/ I_{534} and Hg^{2+} concentration within the range 0–51 μM, demonstrating that **BN-S** was a promising ratiometric

fluorescence probe for the quantitative determination of the Hg^{2+} concentration. The detection limit for Hg^{2+} was calculated to be 72.7 nM at the signal to noise ratio (S/N = 3) from the linear equation (inset of Fig. 4b). The detection limit is comparable to those of other ratiometric fluorescence Hg^{2+} probes,[7] indicating the high sensitivity of **BN-S** for Hg^{2+} sensing. More importantly, the Hg^{2+}-promoted deprotection of **BN-S** takes place in a solvent system consisting of almost pure water, which is one notable advantage over precedent thioacetal-based Hg^{2+} probes.[23]

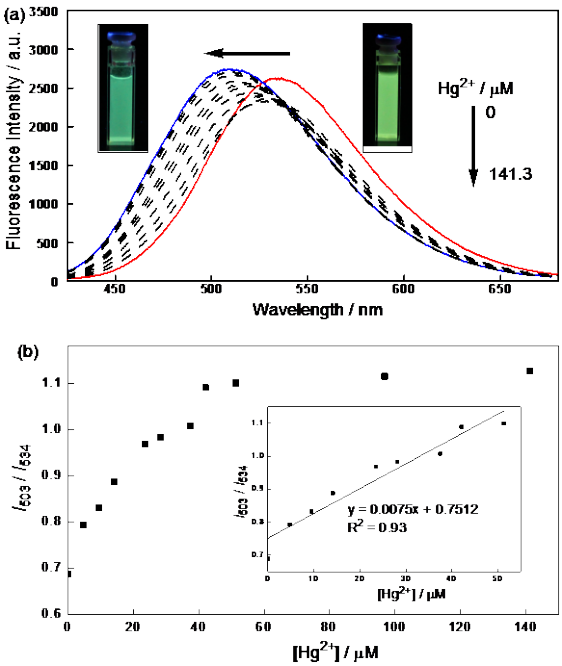

Fig. 5 (a) Fluorescence spectra (λ_{ex} = 350 nm) changes of nano-aggregate of **BN-S** in water (52.6 μM) upon increasing addition of Hg^{2+} (chloride salt). (b) Plot of fluorescence intensity ratios between 503 and 534 nm (I_{503}/ I_{534}) versus concentration of Hg^{2+}. Inset: Linear relation of I_{503}/ I_{534} versus concentration of Hg^{2+} in the range of 0–51 μM.

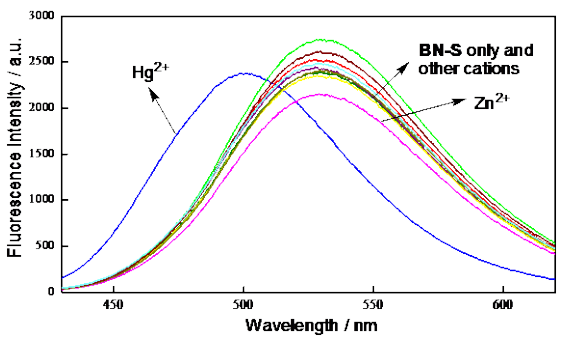

Fig. 6 Fluorescence spectra (λ_{ex} = 320 nm) of nano-aggregates of **BN-S** in water (52.6 μM) upon addition of various metal ions (30 equiv)

In order to enable the probe to work in more complex systems, selectivity is one of the most important performance indexes. To investigate the fluorescence sensing selectivity of **BN-S** towards Hg^{2+}, fluorescence spectra changes of **BN-S** were examined upon addition of various metal cations. As shown in Fig. 6, only the addition of Hg^{2+} caused the blue shift in the emission. The other competitive cations, such as Mg^{2+}, Pb^{2+}, Cu^{2+}, Ba^{2+}, Ca^{2+}, Cd^{2+}, Zn^{2+}, even Ag^{+} only induced slight variations in the fluorescence intensity while the emission maximum wavelengths remain unchanged. Therefore, **BN-S** also displays high selectivity in sensing of Hg^{2+} over other cations.

Optical response of BN-S to F^-

To explore the sensing ability of **BN-S** for F^-, the absorption and emission spectra changes were first examined in THF solution using *n*-Bu_4NF (TBAF) as the fluoride source (Fig. 7). In THF, the absorption and emission maximum wavelengths of **BN-S** were located at 308 and 565 nm, respectively. Upon addition of excess amount of F^-, the absorption at 308 nm weakened dramatically and the emission shifted to 395 nm, demonstrating the efficient complexation of tri-coordinate

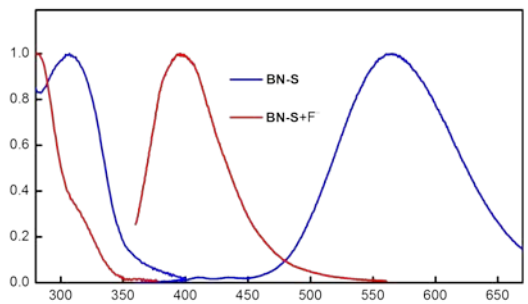

Fig. 7 UV/vis absorption and fluorescence spectra (λ_{ex} = 340 nm) **BN-S** in THF (22.4 μM) in the absence and presence of 5 equiv. of F^- (TBA salt).

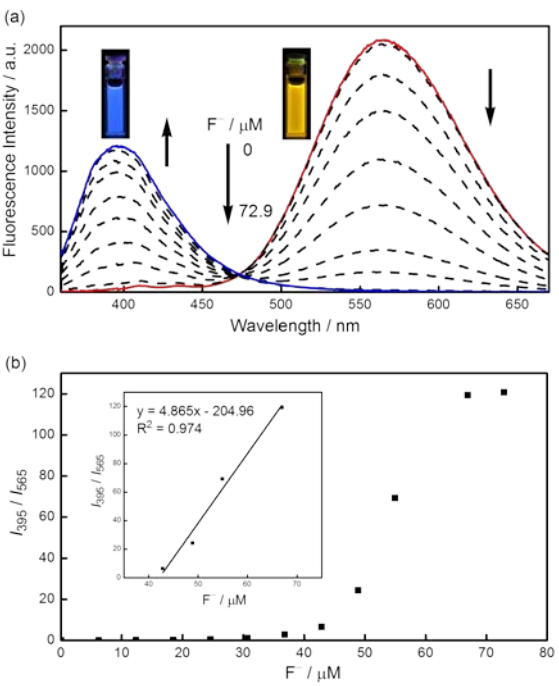

Fig. 8 (a) Fluorescence spectra (λ_{ex} = 340 nm) changes of **BN-S** in THF solution (22.4 μM,) upon increasing addition of F^- (TBA salt). (b) Plot of fluorescence intensity ratios between 395 and 565 nm (I_{395}/ I_{565}) versus concentration of F^-. Inset: Linear relation of I_{395}/ I_{565} versus concentration of F^- in the range of 43–67 μM.

boron center with F^- to form the corresponding complex BN-S•F^-. The complexation of **BN-S** with F^- also leads to the shortening of fluorescence time, which was accompanied by the significant acceleration in radiative and nonradiative decay processes. It was worth noticing that the shift in fluorescence (170 nm) is extremely very large, implying the possible utility of **BN-S** as ratiometric fluorescence probe for F^-. Herein, the fluorescence titration experiment of **BN-S** (22.4 μM) with F^- was next carried out and the fluorescence spectra changes upon addition of F^- are shown in Fig. 8. As the concentration of F^- increased incrementally, the fluorescence band at 565 nm decreased and the hypochromic peak at 395 nm appeared gradually. The ratios of fluorescence intensity at 395 and 565 nm ($I_{395}/_{565}$) exhibit a dramatic change from 0.013 to 120.7 (Figure 8b). In addition, an excellent linear relationship was also observed between $I_{395}/_{565}$ and F^- concentration when F^- concentration ranging from 42.8 μM to 66.9 μM, enabling the quantitative determination of F^- concentration. Intriguingly, the colorimetric F^- sensing by naked eyes is also feasible owing to the dramatic fluorescence color change from yellow to skyblue.

Theoretical calculations

To gain a thorough comprehension of the changes in photophysical properties of **BN-S** upon addition of Hg^{2+} and F^- ions, we conducted theoretical calculations of **BN-S**, **BN-CHO** and **BN-S•F**$^-$ with Gaussian 09 program.[24] Their molecular geometries were first optimized using density functional theory (DFT) at the B3LYP/6-31G(d) level of theory. We also performed time-dependent density-functional theory (TD-DFT) calculations at the B3LYP/6-31G(d) level of theory. The pictorial drawing of their molecular orbitals are shown in Fig. 9, and the calculated data are summarized in Table 2.

The introduction of dithioacetal group exhibits almost no influence on the structure of 2-dimesitylboryl-2'-(N,N-dimethylamino)biphenyl core unit, including the optimized molecular geometry, molecular orbital energy levels and electronic distributions of frontier orbitals.[22] Thus in **BN-S**, both HOMO and HOMO−1 contain contributions from dimethylamino phenyl moiety and one mesityl group. The HOMO is mainly dominated by dimethylamino phenyl moiety while HOMO−1 is mainly dominated by one mesityl group on boron atom. On the contrary, the LUMO is dominantly localized on dimesitylborylphenyl part. Notably, the oscillator strength of the lowest transition (S_1), which mainly consisting

Table 2. Calculated Kohn-Sham molecular orbital energy levels and the calculated vertical excited states for **BN-S**, **BN-CHO** and **BN-S•F**$^-$.

	HOMO−1	HOMO	LUMO	transition	S_1 energy / nm	oscillator strength	transition	S_2 energy / nm	oscillator strength	transition	S_3 energy / nm	oscillator strength
BN-S	−5.77	−5.37	−1.54	H→L (97%)	394	0.0081	H−1→L (88%)	354	0.0514	H−2→L (69%)	339	0.0093
BN-CHO	−5.93	−5.65	−1.64	H→L (96%)	377	0.0199	H−1→L (94%)	348	0.0312	H−2→L (97%)	336	0.0203
BN-S•F$^-$	−2.53	−2.34	2.28	H→L (98%)	304	0.008	H−2→L (88%)	289	0.097	H−1→L (69%)	285	0.0043

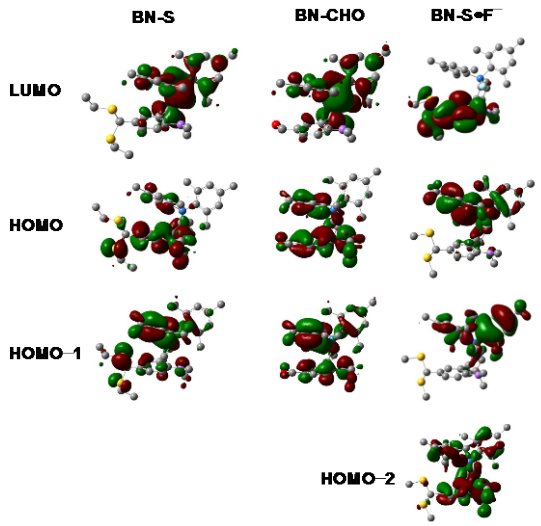

Fig. 9 Associated molecular orbitals that are likely responsible for the low-energy absorption bands of **BN-S**, **BN-CHO** and BN-S•F^-

the enlarged HOMO-LOMO energy gap once transformed to **BN-CHO**.

With regard to influence of complexation of fluoride with **BN-S**, it is most notable that the LUMO is mainly distributed over the phenyl ring attached to amino group. This fact clearly suggest the complete interruption of p_π-π^* conjugation, which leads to the significant elevation in the energy levels of both HOMO and LUMO, especially LUMO. The lowest allowed transition is mainly assignable to the S_2 transition from HOMO−2 delocalized over biphenyl unit and two mesityl group to the LUMO. As a result, it is easily understandable that remarkable blue shift was observed in both absorption and emission of **BN-S** upon addition of fluoride ions. Although the accuracy of the calculated frontier energy levels and the calculated transition energy is not sufficiently high by this level of calculation, these results clearly explain the reason for the optical response of **BN-S** to Hg^{2+} and F^-.

Conclusions

In summary, we have designed and synthesized a triarylborane derivative **BN-S**, derived from 2-dimesitylboryl-2'-(N,N-dimethylamino)biphenyl core skeleton. This compound contains both a Hg^{2+}-responsive dithioacetal group and a F^--responsive boryl group. Hg^{2+}-promoted deprotection of dithioacetal group generates **BN-CHO**, leading to low-lying of HOMO energy level and thus obvious blue shift of fluorescence. In addition, the complexation of fluoride ions with tri-coordinate boron center interrupts the p_π-π^* and thus the intramolecular CT transition, which causes significant blue shift in emission. As a result, **BN-S** can act as a promising ratiometric bifunctional fluorescence probe to detect cationic Hg^{2+} and anionic F^-, simultaneously. It is noteworthy that the ratiometric fluorescence sensing of Hg^{2+} is feasible in an aqueous medium consisting of almost pure water. Despite the extensive utility of triarylboranes as fluoride probe, the examples that act as bifunctional probes are very rare. We have herein provided a successful example of bifunctional ratiometric fluorescence probe and we believe that our current results would give some important basis for the further design of triarylborane-based bifunctional probes to detect fluoride and other ions. Moreover, we also have demonstrated a successful example for the application of 2-dimesitylboryl-2'-(N,N-dimethylamino)biphenyl core skeleton through fine tuning its electronic structure. Further design of functional materials utilizing this skeleton to explore their potential applications in other fields is underway in our group.

Acknowledgements

This work was supported by the National Nature Science Foundation of China (Grants Nos 21072117, 21272141) and Promotive Research Fund for Excellent Young and Middle-aged Scientists of Shandong Province (No BS 2012CL021n).

Experimental

General

Melting points (mp) were measured on a Tektronix XT-4 instrument. ^1H and ^{13}C NMR spectra were recorded with a Bruker 300 spectrometer in $CDCl_3$. High resolution mass spectra (HRMS) were recorded on an Agilent Q-TOF 6510 LC/MS mass spectrometer using the electrospray ionization (ESI) technique. UV−vis absorption and fluorescence spectra measurement were performed with A TU-1901 spectrometer (Beijing Purkinje General Instrument) and a Hitachi F-7000 spectrometer.

Computational methods

The geometries of **BN-S**, **BN-CHO** and **BN-S•F**$^-$ in the ground state were optimized using density functional theory (DFT) at the B3LYP/6-31G(d) level of theory by Gaussian 09 program.[24] All geometry optimizations were followed by a frequency calculation to ensure that the optimized geometry was at a minimum. The time-dependent density functional theory (TD-DFT) calculations were conducted at B3LYP/6-31G(d) level of theory.

Synthesis of BN-S

To a mixture of **BN-CHO** (473 mg, 1 mmol) and P_2O_5/SiO_2 (630 mg) in CH_2Cl_2 (20 ml) was added EtSH (0.6 ml, 8 mmol) under a stream of nitrogen. The reaction mixture was stirred for 24 hours at 40℃ and then a saturated NaCl solution was added. The aqueous layer was extracted with CH_2Cl_2. The combined organic layer was dried over anhydrous Na_2SO_4, filtered, and concentrated under vacuum pressure. The resulting mixture was subjected to a silica gel column chromatography (petroleum ether/CH_2Cl_2, 5/1, R_f = 0.40) to afford 502 mg (0.87 mmol) of **BN-S** in 87% yield as yellowish green solids: mp 149−151 °C; ^1H NMR (300 MHz, $CDCl_3$) δ 7.47−7.55 (m, 2H), 7.27−7.30 (m, 2H), 7.09 (s, 1H), 6.96 (d, J = 5.4 Hz, 1H), 6.43 (d, J = 8.4 Hz, 1H), 6.46 (br, 4H), 4.78 (s, 1H), 2.51–2.69 (m, 4H), 2.31 (br, 6H), 2.17 (br, 6H), 1.90 (s, 12H), 1.25 (t, J = 7.2 Hz, 6H) ppm; ^{13}C NMR (100 MHz, $CDCl_3$) δ 150.7, 148.3, 144.4, 140.5, 137.2, 136.0, 132.2, 131.8, 131.73, 131.3, 127.9, 126.8, 126.4, 115.9, 52.6, 43.7, 25.9, 23.1, 21.1, 14.4 ppm; HRMS (ESI): 580.3210 ($[M+H]^+$); Calcd for $C_{37}H_{47}BNS_2$: 580.3243.

Notes and references

[a] School of Chemistry and Chemical Engineering, Key Laboratory of Special Functional Aggregated Materials, Ministry of Education, Shandong University, Jinan 250100, People's Republic of China.

† Electronic Supplementary Information (ESI) available: ^1H NMR and ^{13}C NMR spectra of compound **BN-S**. See DOI: 10.1039/c000000x/

1 (a) Z. Xu, S. K. Kim and J. Yoon, *Chem. Soc. Rev.*, 2010, **39**, 1457; (b) E. Kimura, *Acc. Chem. Res.*, 2001, **34**, 171.

2 (a) H. Kim, W. Ren, J. Kim and J. Yoon, *Chem. Soc. Rev.*, 2012, **41**, 3210; (b) M.-H. Lee, Z. Zhang, C.-W. Lim, Y.-H. Lee, S. Dongbang, C. Kang and J. S. Kim, *Chem. Rev.*, 2013, **113**, 5071; (c) H. H. Harris, I. J. Pickering and G. N. George, *Science*, 2003, **301**, 1203.

3 P. B. Tchounwou, W. K. Ayensu, N. Ninashvili and D. Sutton, *Environ. Toxicol.*, 2003, **18**, 149.

4 (a) M. A. Holland and L. M. Kozlowski, *Clin. Pharm.*, 1986, **5**, 737; (b) R. J. Carton, *Fluoride*, 2006, **39**, 163.

5 (a) R. H. Dreisbuch, *Handbook of Poisoning*, Lange Medical Publishers, Los Altos, CA, 1980; (b) P. P. Singh, K. Barjatiya, S. Dhing, R. Bhatnagar, S. Kothari and V. Dhar, *Urol. Res.*, 2001, **29**, 238; (c) M. Kleerekoper, *Endocrinol. Metab. Clin. North. Am.*, 1998, **27**, 441.

6 J. R. Lakowicz, *Principles of Fluorescence Spectroscopy*, Springer, New York, 2006.

7 (a) L. N. Neupane, J. M. Kim, C. R. Lohani and K.-H. Lee, *J. Mater. Chem.*, 2012, **22**, 4003; (b) M.-H. Yang, P. Thirupathi and K.-H. Lee, *Org. Lett.*, 2011, **13**, 5028; (c) H. Lee and H. H. Kim, *Tetrahedron Lett.*, 2011, **52**, 4775; (d) H. Li and H. Yan, *J. Phys. Chem. C*, 2009, **113**, 7526; (e) A. Dhir, V. Bhalla and M. Kumar, *Org. Lett.*, 2008, **10**, 4891.

8 (a) C. Saravanan, S. Easwarmoorthi, C.-Y. Hsiow, K. Wang, M. Hayashi and L. Wang, *Org. Lett.*, 2014, **16**, 354; (b) X.-M. Liu, Y.-P. Li, Y.-H. Zhang, Q. Zhao, W.-C. Song, J. Xu and X.-H. Bu, *Talanta*, 2015, **131**, 597; (c) E. J. Jun, Z. Xu, M. Lee and J. Yoon, *Tetrahedron Lett.*, 2013, **54**, 2755; (d) L. Gai, H. Chen, B. Zhou, H. Lu, G. Lai, Z. Li and Z. Shen, *Chem. Commun*., 2012, **48**, 10721. (e) J.-F. Zhang, C. S. Lim, S. Bhuniya, B. R. Cho and J. S. Kim, *Org. Lett.*, 2011, **13**, 1190;

9 (a) M. Kumar, R. Kumar and V. Bhala, *Chem. Commun.*, 2009, 7384; (b) P. G. Sutariya, N. R. Modi, A. Pandya, B. K. Joshi, K. V. Joshi and S. K. Menon, *Analyst*, 2012, **137**, 5491; (c) D. Maity and T. Govindaraju, *Chem. Commun.*, 2012, **48**, 1039; (d) P. N. Basa and A. G. Sykes, *J. Org. Chem.*, 2012, **77**, 8428; (e) E. Karakus, M. Üçüncüs and M. Emrullahoğlu, *Chem. Commun*., 2014, **50**, 1119.

10 (a) B. Paramanik, S. Bhattacharyya and A. Patra, *Chem. Eur. J*., 2013, **19**, 5980; (b) N. Kumari, N. Dey and S. Bhattacharya, *Analyst*, 2014, **139**, 2370; (c) N. R. Chereddy, P. Nagaraju, M. V. N. Raju, K. Saranraj, S. Thennarasu and V. J. Rao, *Dyes and Pigments*, 2015, **112**, 201.

11 (a) C. R. Wade, A. E. J. Broomsgrove, S. Aldridge and F. P. Gabbaï, *Chem. Rev.*, 2010, **110**, 3958; (b) T. W. Hudnall, C.-W. Chiu and F. P. Gabbaï, *Acc. Chem. Res.*, 2009, **42**, 388; (c) Z. M. Hudson and S. Wang, *Acc. Chem. Res*., 2009, **42**, 1584.

12 (a) F. Jäkel, *Chem. Rev.*, 2010, **110**, 3985; (b) M. Elbing and G. C. Bazan, *Angew. Chem. Int. Ed.*, 2008, **47**, 834; (c) S. Yamaguchi and A. Wakamiya, *Pure Appl. Chem.*, 2006, **78**, 1413; (d) C. D. Entwistle and T. B. Marder, *Chem. Mater*., 2004, **16**, 4574; (e) C. D. Entwistle and T. B. Marder, *Angew. Chem. Int. Ed.*, 2002, **41**, 2927.

13 (a) S. Yamaguchi, S. Akiyama and K. Tamao, *J. Am. Chem. Soc.*, 2001, **123**, 11372; (b) Y. Kubo, M. Yamamoto, M. Ikeda, M. Takeuchi, S. Shinkai, S. Yamaguchi and K. Tamao, *Angew. Chem. Int. Ed.*, 2003, **42**, 2036.

14 (a) C.-W. Chiu and F. P. Gabbaï, *J. Am. Chem. Soc*., 2006, **128**, 14248; (b) H. Zhao and F. P. Gabbaï, *Org. Lett.*, 2011, **13**, 1444; (c) C. R. Wade and F. P. Gabbaï, *Dalton Trans.*, 2009, **42**, 9169.

15 (a) X.-Y. Liu, D.-R. Bai and S. Wang, *Angew. Chem. Int. Ed.*, 2006, **45**, 5475; (b) Z. M. Hudson, X.-Y. Liu and S. Wang, *Org. Lett.*, 2011, **13**, 300.

16 (a) P. K. Chen and F. Jäkle, *J. Am. Chem. Soc.*, 2011, **133**, 20142; (b) H. Li, R. A. Lalancette and F. Jäkle, *Chem. Commun.*, 2011, **47**, 9378.

17 (a) Y.-H. Zhao, H. Pan, G.-L. Fu, J.-M. Lin and C.-H. Zhao, *Tetrahedron Lett.*, 2011, **52**, 3832; (b) G.-L. Fu, H. Pan, Y.-H. Zhao and C.-H. Zhao, *Org. Biomol. Chem.*, 2011, **9**, 8141; (c) H. Sun, X. Dong, S. Liu, Q. Zhao, X. Mou, H. Y. Yang and W. Huang, *J. Phys. Chem. C*, 2011, **115**, 19947.

18 (a) Z.-Q. Liu, M. Shi, F.-Y. Li, Q. Fang, Z.-H. Chen, T. Yi and C. H. Huang, *Org. Lett.*, 2005, **7**, 5481; (b) D.-X. Cao, Z.-Q. Liu and G.-Z. Li, *Snes. Actutators, B: Chemical*, 2008, **133**, 489; (c) M.-S. Yuan, Q. Wang, W. Wang, D.-E. Wang, J. Wang and J. Wang, *Analyst*, 2014, **139**, 1541.

19 (a) S. K. Sarkar and O. Thilagar, *Chem. Commun*., 2013, **49**, 8558; (b) P. C. A. Swamy, S. Mukherjee and P. Thilagar, *Chem. Commun.*, 2013, **49**, 993; (c) P. C. A. Swamy, R. N. Priyanka and P. Thilagar, *Dalton Trans.*, 2014, **43**, 4067; (d) G. R. Kumar and P. Thilagar, *Dalton Trans*., 2014, **43**, 7200.

20 (a) W.-J. Xu, S.-J. Liu, X. Zhao, N. Zhao, Z.-Q. Liu, H. Xu, H. Liang, Q. Zhao, X.-Q. Xu and W. Huang, *Chem. Eur. J.* 2013, **19**, 621; (b) W. J. Xu, S.-J. Liu, X.-Y. Zhao, S. Sun, S. Cheng, T.-C. Ma, H.-B. Sun, Q. Zhao and W. Huang, *Chem. Eur. J.* 2010, **16**, 7125; (c) W. Xu, S. Liu, H. Sun, X. Zhao, Q. Zhao, S. Sun, S. Cheng, T. Ma, L. Zhou and W. Huang, *J. Mater. Chem.* 2011, **21**, 7572; (d) Q. Zhao, F. Li, S. Liu, M. Yu, Z. Liu and C. Huang, *Inorg. Chem.* 2008, **47**, 9256.

21 (a) X. He and V. W.-W. Yam, *Org. Lett.*, 2011, **13**, 2172; (b) Z. Yin, A. Y.-Y. Tam, K. M.-C. Wong, C.-H. Tao, B. Li, C.-T. Poon, L. Wu and V. W.-W. Yam, *Dalton Trans*., 2012, **41**, 11340; (c) Y.-H. Lee, N. V. Nghia, M. J. Go, J. Lee, S. U. Lee and M.-H. Lee, *Organometallics*, 2014, **33**, 753. (d) D.-M. Chen, S. Wang, H.-X. Li and X.-Z. Zhu and C.-H. Zhao, *Inorg. Chem*., 2014, **53**, 12532.

22 (a) H. Pan, G.-L. Fu, Y.-H. Zhao and C.-H. Zhao, *Org. Lett.*, 2011, **13**, 4830; (b) Y.-Q. Yan, Y.-B. Li, J.-W. Wang and C.-H. Zhao, *Chem. Asian J.*, 2013, **8**, 3164; (c) C. Wang, J. Jia, W.-N. Zhang, H.-Y. Zhang and C.-H. Zhao, *Chem. Eur. J*., 2014, **20**, 16590.

23 (a) S. Yang, W. Yang, Q. Guo, T. Zhang, K. Wu and Y. Hu, *Tetrahedron*, 2014, **70**, 8914; (b) F. Lu, M. Yamamura and T. Nabeshima, *Dalton Trans.*, 2013, **42**, 12093; (c) A. K. Mahapatra, R. Maji and P. Sahoo, *Tetrahedron Lett*., 2012, **53**, 7031.

24 Gaussian 09, Revision A.02, M. J. Frisch, G. W. Trucks, H. B. Schlegel, G. E. Scuseria, M. A. Robb, J. R. Cheeseman, G. Scalmani, V. Barone, B. Mennucci, G. A. Petersson, H. Nakatsuji, M. Caricato, X. Li, H. P. Hratchian, A. F. Izmaylov, J. Bloino, G. Zheng, J. L. Sonnenberg, M. Hada, M. Ehara, K. Toyota, R. Fukuda, J. Hasegawa, M. Ishida, T. Nakajima, Y. Honda, O. Kitao, H. Nakai, T. Vreven, J. A. Montgomery, Jr., J. E. Peralta, F. Ogliaro, M. Bearpark, J. J. Heyd, E. Brothers, K. N. Kudin, V. N. Staroverov, R. Kobayashi, J. Normand, K. Raghavachari, A. Rendell, J. C. Burant, S. S. Iyengar, J. Tomasi, M. Cossi, N. Rega, J. M. Millam, M. Klene, J. E. Knox, J. B. Cross, V. Bakken, C. Adamo, J. Jaramillo, R. Gomperts, R. E. Stratmann, O. Yazyev, A. J. Austin, R. Cammi, C. Pomelli, J. W. Ochterski, R. L. Martin, K. Morokuma, V. G. Zakrzewski, G. A. Voth, P. Salvador, J. J. Dannenberg, S. Dapprich, A. D. Daniels, O. Farkas, J. B. Foresman, J. V. Ortiz, J. Cioslowski, and D. J. Fox, Gaussian, Inc., Wallingford CT, 2009.